N87-22606

AIRCRAFT APPROACH GUIDANCE USING RELATIVE LORAN-C NAVIGATION

Antonio L. Elias
Flight Transportation Laboratory
Massachusetts Institute of Technology
Cambridge, Massachusetts

PRECEDING PAGE BLANK NOT FILMED

The experiments carried out during 1984 at MIT focused on two aspects of LORAN-C relative navigation that will impact system performance at the sub-microsecond level of accuracy: tracking loop bandwidth and localized field deformations. Figures 1 to 3 show the result of a basic experiment illustrating both these effects. A Micrologic Model 3000 receiver mounted on a vehicle is accelerated to a constant speed and then decelerated to a full stop between points A and B. After a 2-minute pause, the vehicle is reversed and the maneuver repeated in the opposite direction from points C to D. The first measured set of TD's in the sample was taken as the definition of point "A", and all subsequent positions plotted relative to this datum. Features of interest in Figure 1 include: a) the random noise in the plotted position is sufficiently low to discern the 10-m width of the road over which the test was performed; b) the navigated position overshoots the actual position during braking (and lags it during acceleration); and c) a reduction in signal-to-noise ratio (SNR), as occurred at the end of the run while the vehicle was standing at point D, substantially increases the navigated position random noise.

The effect of vehicle acceleration and deceleration is better seen in the plot of Figure 2; here, measured and position-derived TD's are plotted against time. As can be seen, the tracking loops can be very well approximated by second-order linear systems, in spite of the discrete digital implementation used in this receiver. The trade-off between random noise and lag/overshoot in the navigated position implied by selection of the tracking loop bandwidth is illustrated in Figure 3, where the test of Figure 1 is repeated with a tracking loop filter bandwidth four times larger than that used in Figure 1.

If the tracking loops can be modeled as simple second-order linear systems with constant damping ratio (0 to 5 was assumed after Figure 2), then it is possible to determine analytically what the root mean square of the random component of time difference will be as a function of filter bandwidth. Figure 4 shows this relationship, where the filter is characterized by its time constant and acceleration gain $\left(\text{-3dB bandwidth} = \omega = \frac{1}{\pi}\sqrt{K_A},\ \tau = \frac{1}{\sqrt{K_A}} = \frac{1}{\pi\omega}\right)$. Also plotted in Figure 4 are some experimental points obtained with the Micrologic 3000 receiver in a single, stationary location with various levels of SNR and two tracking loop bandwidths. As it can be seen, there is general agreement between experimental results and the simple linear model.

Such simple linear models, if assumed valid, can then be used to optimize the tradeoff between acceleration-induced errors, which increase with reduced tracking loop bandwidth, and the random component of TD, which increases with increased tracking loop bandwidth. Figure 5 shows the 2-σ TD error versus SNR, resulting from choosing a bandwidth such that the acceleration-induced bias (at the level of acceleration indicated by the curve label) equals the 2-σ TD random noise at each SNR value. Marked along the curves are the optimal loop gains in each case. As can be seen, the resulting system performance is significantly lower than that which would be expected from a cursory look at Figure 4 (0.1 μsec is approximately 60 feet or 20 meters).

Performance at the sub-microsecond level of accuracy, as seems to be feasible in view of the results of Figure 5, requires that the Loran-C signal field itself be consistent to that accuracy in the area around the datum point in which operations will be carried out. A survey of measured TD's in the vicinity of Hanscom AFB, MA, indicates that there may be local distortions in the stationary Loran-C electromagnetic field much larger than 1 microsecond. Figure 6 shows vector differences between TD-derived and map-derived antenna positions around the base; the reference

TD's were selected so as to zero the sum of these vector differences, and thus can be interpreted as an "area average" ASF correction. Figure 7 summarizes those vector differences in a single plot; of interest is that the dispersion seems largest in the direction of the gradient of the second pair of stations, which happen to have the largest SNR in the area. As it can be seen, the 2-σ error is about 1 microsecond.

It was postulated that these large stationary differences might have been caused by large terrain features, metallic structures (e.g. hangars) and CW interference (e.g. power lines) in the area. Thus a second set of experiments, depicted in Figure 8, was carried out over a flat, obstacle-free area. Two hundred and eighty data points were taken at each location in a grid 300 ft by 200 ft in side, at 100 feet intervals. The resulting sampling error of estimate of the mean of each sample is less than 1 m. As can be seen, the differences between actual and (averaged) measured position are of the order of 10 to 20 meters (the point with zero difference was taken as the "anchor point" and the average TD's used as the reference TD's). We have labeled this repeatable distortion field "microdeformation" and intend to further explore this effect, both at ground level and at altitude, using NASA-supplied kitoons (kite-balloons).

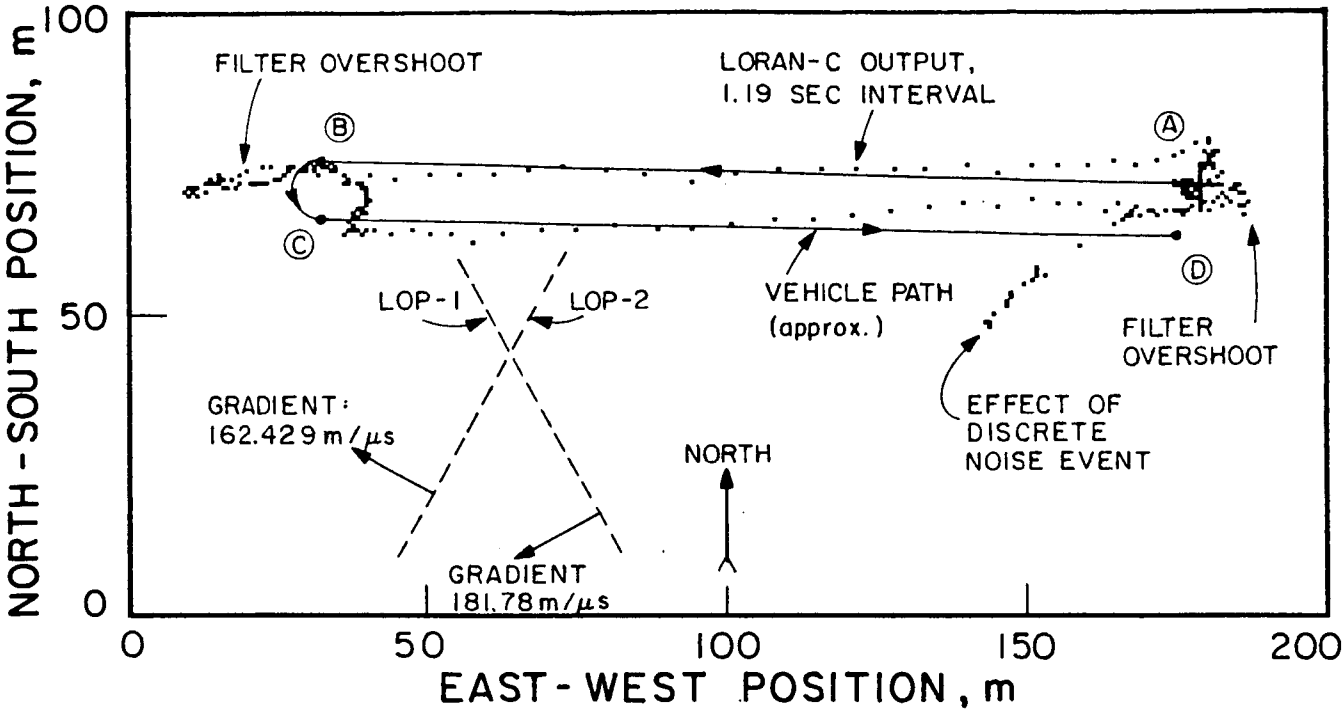

Figure 1. Vehicle-mounted relative Loran-C test (loop time constant was 18 seconds).

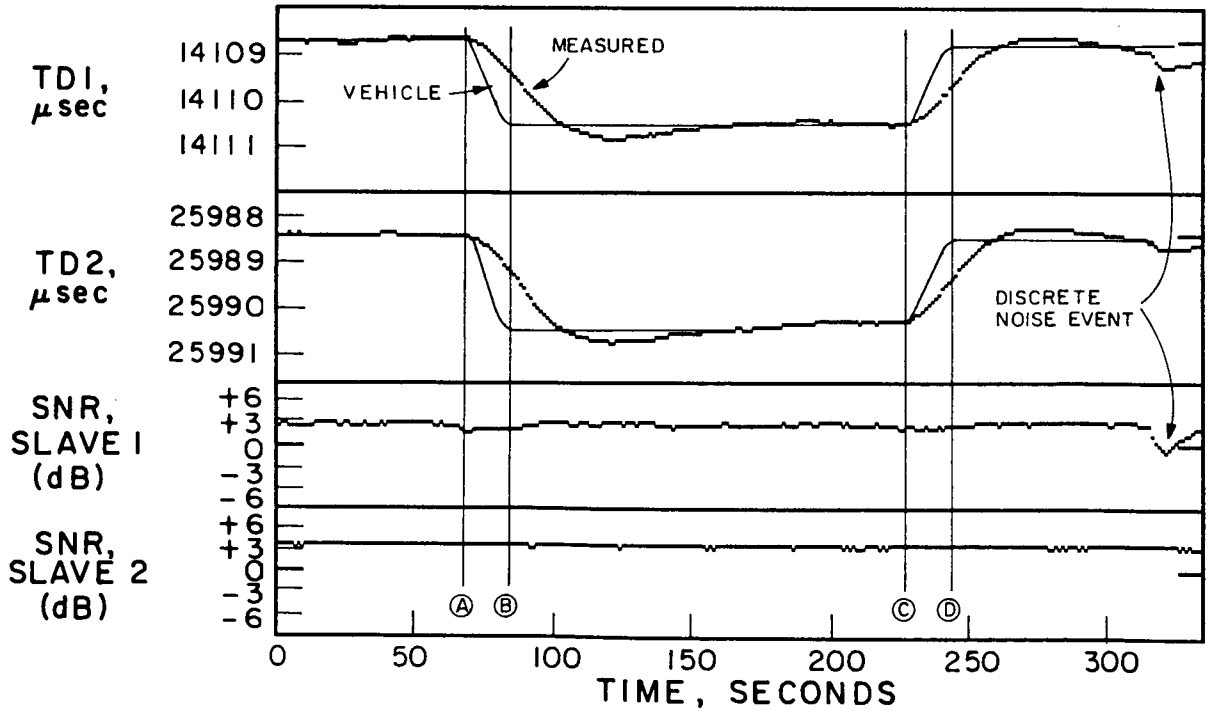

Figure 2. Measured and theoretical time differences and measured SNR's for the test of Figure 1.

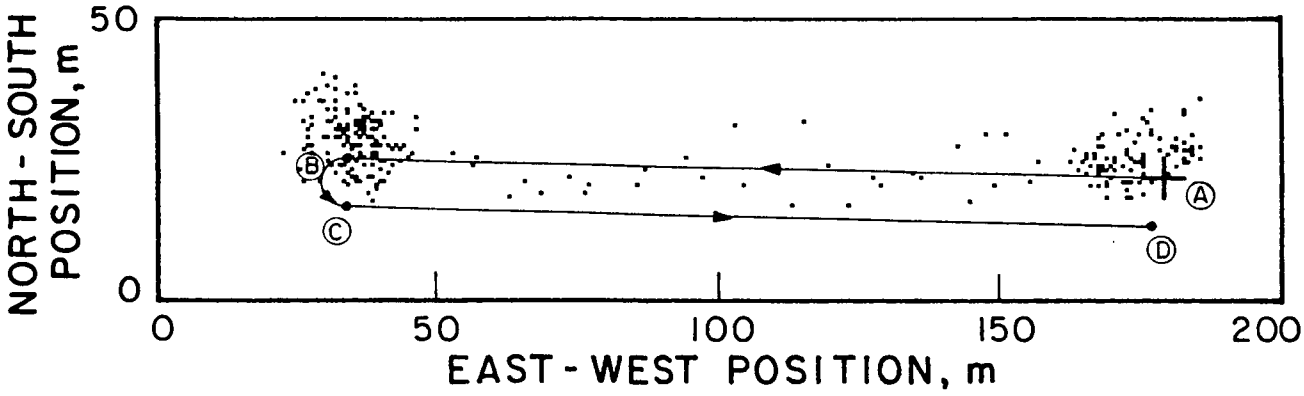

Figure 3. Vehicle-mounted test (loop time constant was 4 seconds).

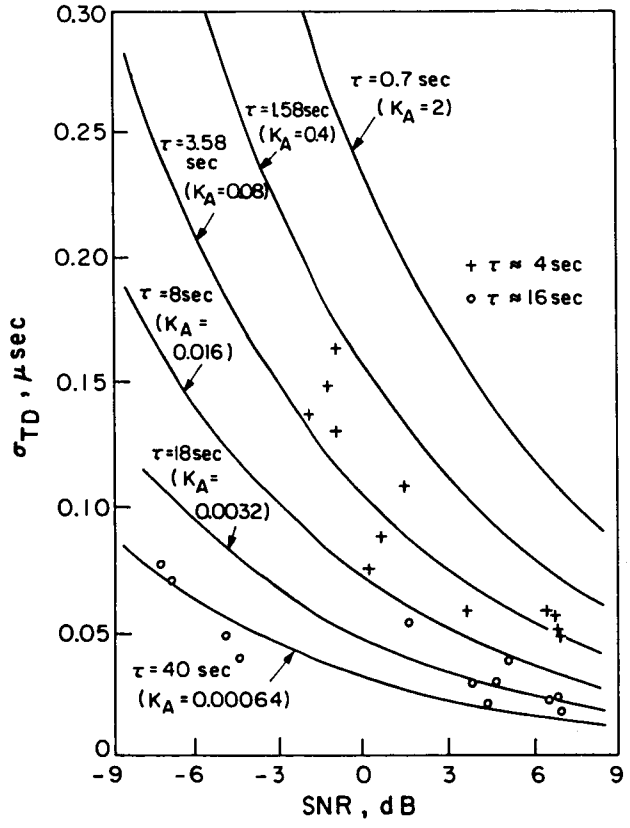

Figure 4. Theoretical and measured time difference variances as a function of SNR for various loop time constants.

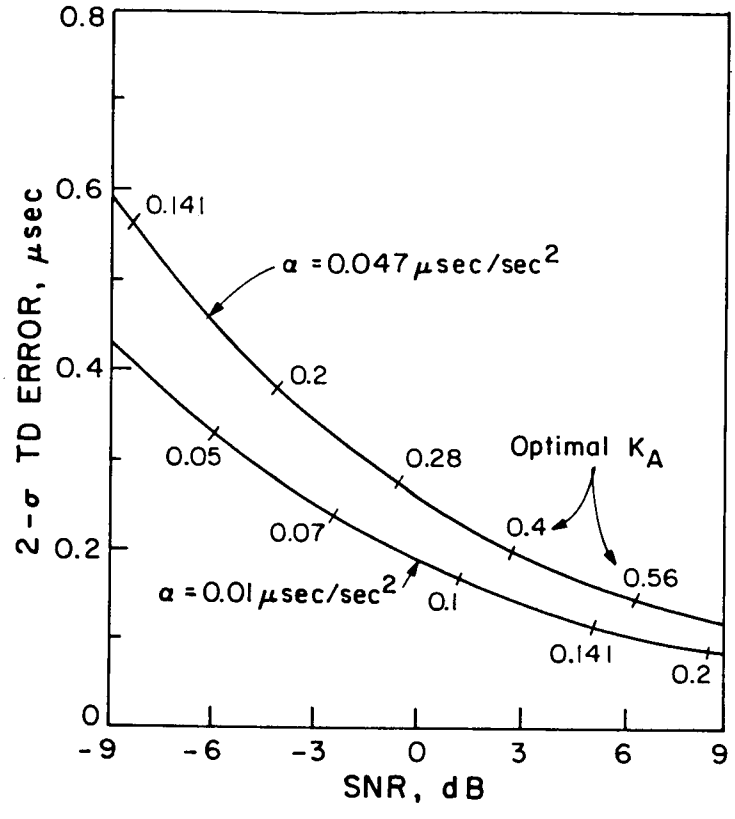

Figure 5. The 2-σ error as a function of SNR for balanced-design loop time constants.

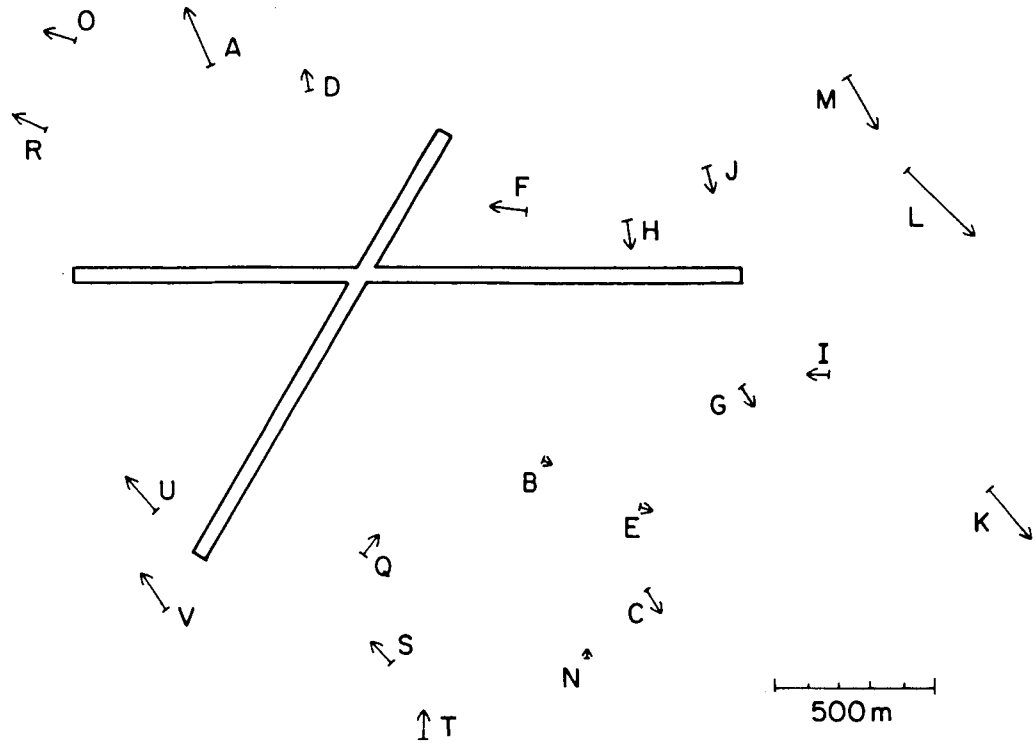

Figure 6. Differences between actual and relative Loran-C derived positions around Hanscom AFB, MA.

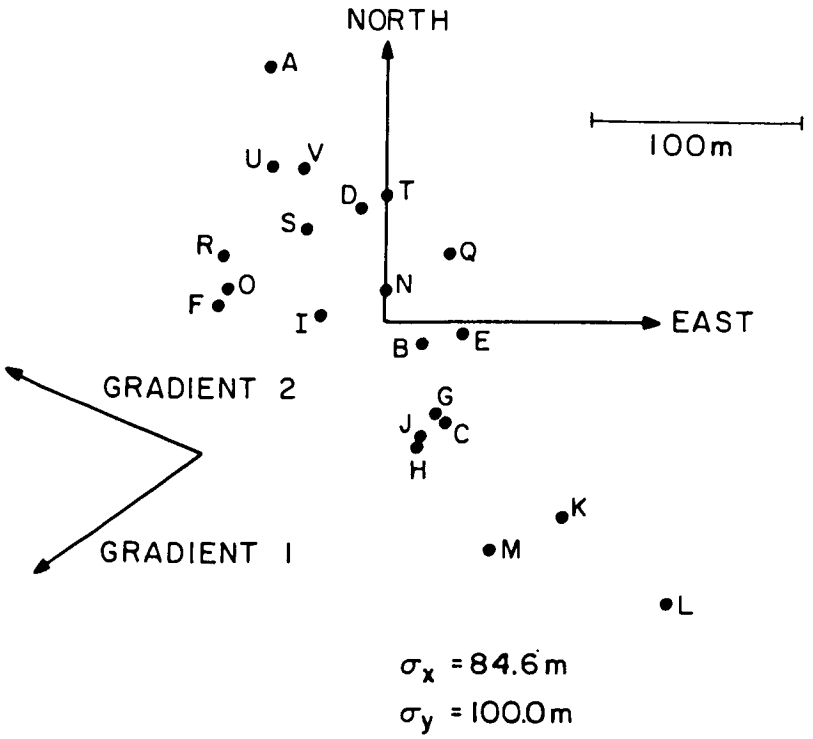

Figure 7. Distribution of the position errors of Figure 6.

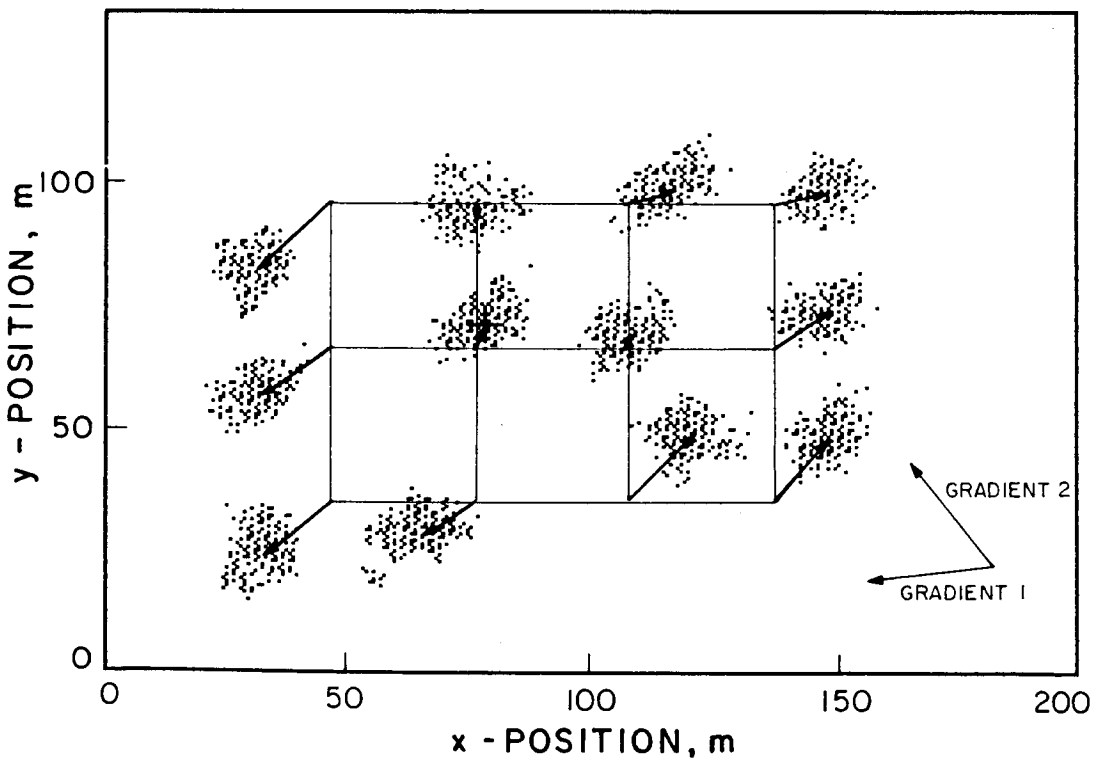

Figure 8. Actual and relative Loran-C derived position over open terrain.